Dissipative spatiotemporal soliton in a driven waveguide laser

VLADIMIR L. KALASHNIKOV[1,*], EVGENI SOROKIN[2,3], AND IRINA T. SOROKINA[1,3]

[1] Department of Physics, Norwegian University of Science and Technology, Trondheim, 7491 Norway
[2] Institut für Photonik, TU Wien, Gusshausstrasse 27/387, 1040 Vienna, Austria
[3] ATLA lasers AS, Richard Birkelands vei 2B, 7034 Trondheim, Norway
[*] vladimir.kalashnikov@ntnu.no

Compiled February 22, 2024

A distributed Kerr-lens mode locking regime can be realized in a waveguide laser by spatial profiling of the pump beam, thus creating a spatio-temporal soliton. Additional slow temporal modulation of the pump source stabilizes the spatio-temporal solution in a broad range of parameters, which are defined by the dynamic gain saturation. We choose a Cr:ZnS waveguide laser as a practical example, but such a regime is feasible in various waveguide and fiber oscillators. A far-reaching analogy with Bose-Einstein condensates allows using this approach to stabilization of the weakly dissipative BECs.

http://dx.doi.org/10.1364/ao.XX.XXXXXX

1. INTRODUCTION

The unprecedented progress in the field of mesoscopic physics in its general context, which comprises control of macro-quantum states like Bose-Einstein condensate (BEC) [1–4] and quantum supersolids [5], plasma and turbulence [6–8], attosecond [9], relativistic and high-energy physics [10–13], metaphorical modeling and quantum computations [14–17], physics of ultra-strongly coupled light-matter systems [18], nano-processing [19–21], and other ranges of science, medicine, and technology, became feasible due to the growth understanding of strongly nonlinear phenomena in far-from-equilibrium systems [22, 23]. The coherent, self-organized, and well-localized patterns, namely solitons, play a crucial role in most of these phenomena. The class of such structures, *dissipative solitons* (DSs), is particularly important because DS develops in open systems, where energy exchange with an environment defines its integrity, stability, and coherence [24, 25]. In photonics, DSs are a road to generating ultrafast, robust, and energy-scalable pulses in mode-locked lasers [26, 27] bringing a high-field physics on tabletops of a mid-level university lab [12, 28].

The modern tendencies in generating and exploring laser DSs are based on a controllable enhancement of self-organizing effects induced by nonlinearities and affected both temporal and spatial degrees of freedom [23]. A partial realization of this concept is a *distributed Kerr-lens mode-locking* (DKLM) [29–31]. In a solid-state laser, this technique uses a nonlinear medium that affects a laser beam via self-focusing, thereby changing an effective gain in a laser resonator [32]. The transversal spatial structure of a field in this type of device is close to a fundamental mode of laser oscillator and, thus, trivial, so only longitudinal modes need synchronization. A remarkable breakthrough in energy scalability of such oscillators was demonstrated in both anomalous and normal group-delay dispersion regimes (ADR and NDR, respectively) [30, 33, 34]. It was found that such broad-range scalability could be explained by energy out/in-flows induced by the nontrivial phase structure of DS [27, 35], and the underlying theory of the DS resonance (DSR) [36] were developed.

Using DS in the NDR fiber lasers [37] exploits the enhanced and well-controllable nonlinearities. That bridges fiber and solid-state ultrafast laser photonics [23]. The keystone is utilizing a nonlinear propagation of many interacting spatial modes (e.g., in the so-called multimode fibers, MMF) [38, 39]. Such a nonlinear spatial mode coupling could be caused by nonlinear refraction (or attractive boson interaction in BEC [4]) characterized by the coefficient n_2. A "confining potential" defined by spatial-dependent refractive index $n(x,y)$ ("graded refractive index fibers," or GRIN, nonlinear lattices [40, 41], or laser-induced confinement in BEC) enhances the relaxation of the higher-order modes to a ground-state, i.e., lowest-order spatial mode.

In this work, we propose utilizing a nonlinear mode condensation for DKML aimed at a *spatio-temporal mode-locking* (STML) [42, 43].

Such an approach utilizes a dissipative (i.e., $\Im[n(x,y)] \neq 0$, where n is, e.g., a complex index of refraction in optics) trapping potential [44] for a spatiotemporal DS (STDS) without involving other nonlinear dissipative processes. The 2D dissipative potential, unlike that in Refs. [45, 46] transversal (x,y)-confinement induced by a complex $n(x,y)$ can be associated with a so-called "cigar-type" trapping potential in a weakly dissipative BEC or GRIN (see Table 1) [15]. Then, an evolutionary ("slow") coordi-

Table 1. Correspondences between photonics and BEC [15]

Laser		BEC
Propagation coordinate Z	$\leftrightarrow$	time T
Pulse local time t	$\leftrightarrow$	third spatial coordinate z
Diffraction + anomalous GDD	$\leftrightarrow$	boson kinetic energy
Kerr-nonlinearity	$\leftrightarrow$	boson attractive colliding potential
GRIN	$\leftrightarrow$	cigar-like $(x,\ y)$ trapping potential
Non-selective loss	$\leftrightarrow$	homogeneous BEC dissipation
Graded gain + local time modulation	$\leftrightarrow$	pancake (x,y,z)-shaped inflow of bosons
Spectral dissipation	$\Leftrightarrow$	"kinetic cooling"

nate T is associated with time for BEC or propagation distance Z in a fiber or cavity round-trip in a laser.

A further step is to introduce "longitudinal" ("slow" time T-dependent, or propagation length Z-dependent) modulation of $\Re[n(x,y,T)]$ (or $\Re[n(x,y,Z])$, which is one of the management techniques stabilizing an ST soliton in BEC [47]. In a mode-locked laser, it is also possible to identify a "fast" coordinate (local time t) associated with the frame co-moving with a soliton. The dependence of trapping potential on that coordinate allows a 3D confinement corresponding to a "pancake-like" potential in BEC. In a laser, this corresponds to an active mode-locking driven by an external synchronous phase modulation[48–50], which varies as $\Re[\Delta n(t)] \propto \cos(2\pi t/T_R)$, where T_R is a cavity round-trip period. This modulation is slow (pulse duration τ_p is much shorter than T_R) and can be described by $\Re[\Delta n(t)] \propto t^2 + \text{H.O.T.}$. It was found that such a modulation stabilizes a driven cavity DS [51, 52] and STDS [53]. Here, we intend to exploit a concept of 3D *dissipative* confinement to develop a spatiotemporal mode-locking mechanism to generate stable and energy-scalable STDS ("light bullet"). This technique can be considered as a road to forming a stable mass-scalable STDS in BEC and pattern formation in dissipative turbulent systems, which could be modeled by the dissipative version of the Gross-Pitaevskii equation (GPE) [4, 54]. In contrast to [53, 55], a transversely graded dissipation (i.e., $\Im[n(x,y)] \neq 0$) will be supplemented by dissipative trapping along t-coordinate ($\Im[n(t) \neq 0$), which is a result of periodical loss modulation (or synchronous pumping) synchronized with the laser cavity round-trip. For BEC, this corresponds to a "pancake-like" dissipative confining potential.

2. A "SOFT-APERTURE" DKLM LASER

A. Model

Let us consider a waveguide laser composed of a fiber or crystalline waveguide active medium enclosed in a Fabri-Perót or ring resonator and driven by a pump beam with a parabolic-like transverse $G(x,y)-$ profile and a pump intensity varying with time t at the frequency synchronized with a laser repetition rate. The $t-$coordinate corresponds to a "local time" (in a coordinate

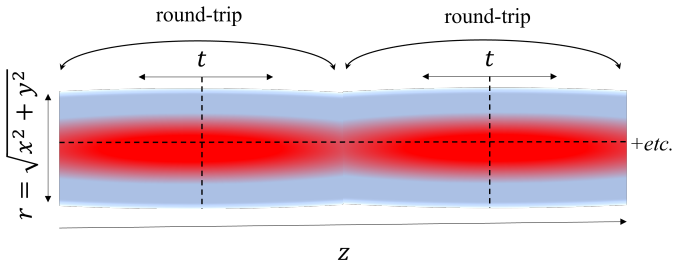

Fig. 1. Multi-scale scheme with a local-time coordinate t synchronized with an STDS group velocity and a global evaluation coordinate Z (see Table 1). The gain (filled by a red) is profiled along the radial coordinate r and the local time t. The last is synchronized with a laser round-trip period.

frame co-moving with an STDS) in photonics or to a longitudinal space coordinate for BEC (see Fig. 1 and Table 1) [15].

Such pump beam acts as a "soft aperture" guiding the laser beam and controlling ("cleaning") its mode structure so that a laser field $a(z,x,y,t)$ tends to condensate into a lowest-order mode. Simultaneously, $t-$modulation provides confinement in the time domain. Thus, this scheme corresponds to a three-dimensional ("pancake-like") dissipative confinement for a BEC or a hybrid mode-locking under synchronous pumping or an active assisting mode locking by synchronous loss modulation [50, 52, 56, 57].

For modeling a (3D+1)-dimensional trapped STDS, we use a distributed model describing the evolution of the (z,x,y,t)-dependent field a propagating along the z-axis (see Table 1 for comparison with BEC) of an active waveguide with the linear and nonlinear refractive indexes $n(x,y)$ and n_2, respectively. Under the action of (x,y,t)-graded pump (Fig. 1), the evolution can be described by a sort of the driven nonlinear Helmholtz equation:

$$-\left[\frac{1}{2k_0n_0}\left(\Delta_{x,y}-\frac{\partial^2}{\partial z^2}\right)+(\frac{\beta_2}{2}-i\tau)\frac{\partial^2}{\partial t^2}\right]a= \tag{1}$$
$$\left[\frac{k_0}{2n_0}\left(n(x,y)^2-n_0^2\right)\right)+i\left(L-G(x,y,t)\right)+k_0n_2\left|a\right|^2+i\frac{\partial}{\partial z}\Bigg]a,$$

where $\Delta_{x,y}$ is a Laplace operator in the Cartesian coordinates, n_0 is a waveguide cladding refractive index, k_0 is a free-space wave number, and the second-order derivative over z contributes only for large beam numerical apertures NA [58, 59]. The terms in Eq. 1 define: (I) – diffraction, (II) – group-delay dispersion with the coefficient β_2, (III) – spectral dissipation with the squared inverse bandwidth τ, (IV) – trapping potential induced by GRIN, (V) – (x,y,t)- graded saturated gain with the coefficient G and linear net-loss L, and (VI) – Kerr-nonlinearity. One has to emphasize the decisive contribution of a saturable and transversely profiled gain $G(x,y,t)$ in Eq. (1).

For a low NA, one may omit the $\frac{\partial^2}{\partial z^2}$-term in Eq. (1). That leads to the nonlinear driven Schrödinger, or the Lugiato-Lefever equation (LLE), which is a test bed model for the study of solitons and non-equilibrium patterns in driven Kerr resonators, micro-cavity and fiber lasers, VCSEL, etc. [60–63].

The rescaling $\psi = a\exp(-iV_0z)$ ($V_0 = (k_0/2n_0)(n_1^2-n_0^2)$, and n_1 is a waveguide core refractive index) leads to the dimensionless mean-field LLE [64–66]:

$$i\frac{\partial\psi\left(Z,X,Y,t'\right)}{\partial Z}=\left\{-\frac{1}{2}\left[\frac{\partial^2}{\partial X^2}+\frac{\partial^2}{\partial Y^2}+\frac{\partial^2}{\partial t'^2}-2i\tau\frac{\partial^2}{\partial t'^2}\right]\right\}\psi+\left\{\left(X^2+Y^2\right)-|\psi|^2-i\left[\Lambda+\kappa(X^2+Y^2)+\omega t'^2\right]\right\}\psi, \quad (2)$$

for the normalizations shown in Table 2 [64, 67].

The dimensional extension by the "fast-time" (or "local time") coordinate t' allows describing the pulse dynamics in the co-moving frame (Z, X, Y, t'). Since an ultrashort pulse is sensitive to a group-delay dispersion (GDD), it has to be taken into account by including the β_2-term in Eq. (1). The normalized version (2) assumes an anomalous net-GDD.

In this work, we assume the parabolic-like transverse profile of the gain beam with the size. Such transversely confined nonlinear gain acts as a "soft aperture" with an effective size $\approx w_p\sqrt{G_0-\Lambda}$ (Table 2). Our model introduces a gain modulation along the $t-$axis described in a parabolic approximation by the modulation coefficient ω [50, 57]. The last resembles the mechanism of the so-called active mode-locking (AM) [68]. In contrast to [53], the proposed method does not use additional phase modulation but only a pumping pulse train synchronized with a resonator period. For simplicity, we manipulate with a graded saturated gain $G(X,Y,t)=G(0,0,0)\times\left[1-\kappa(X^2+Y^2)-\omega t'^2\right]$, where $G(0,0,0)$ or G_0 (see Table 2) corresponds to a saturated gain along a waveguide axis at $t'=0$, and $\kappa=G_0w_p^{-2}$, $\omega=G_0\mathscr{T}^{-2}$ ($\mathscr{T}$ is a "pump pulse duration"). Such an approximation is valid under the condition of quasi-steady state operation of a laser in the vicinity of the lasing threshold, where the saturated net-loss coefficient $\Lambda'=L-G_0$ is close to zero [55].

Another essential factor in Eqs. (1,2) is a spectral dissipation described by the parameter τ. This parameter is inversely proportional to a squared spectral width of the gain band or spectral filter (Table 2).

Thus, one may treat the resulting equation (2) as a dissipative extension of the driven Gross-Pitaevskii equation, which is a well-known tool for analyzing trapped BEC (Table 1) [4].

B. Variational approximation

The study of STDS of Eq. (2) is based on analytical and numerical approaches. The first uses the well-known variational approximation (VA) [55]. The generating Lagrangian for a non-dissipative part of (2) is

$$\mathscr{L}=\frac{i}{2}\left(\psi^*\partial_Z\psi-\psi\partial_Z\psi^*\right)+\frac{1}{2}\left(|\partial_X\psi|^2+|\partial_Y\psi|^2+|\partial_{t'}\psi|^2\right)-|\psi|^4+\left(X^2+Y^2\right)|\psi|^2. \quad (3)$$

The dissipative factors can be described in the form of a "force" source term

$$\mathcal{Q}=-i\left[\Lambda'+\kappa(X^2+Y^2)+\omega t'^2-\tau\frac{\partial^2}{\partial t'^2}\right]\psi \quad (4)$$

in the Euler-Lagrange equation

$$\frac{\partial\int_{-\infty}^{\infty}\mathscr{L}dt'}{\partial\mathbf{f}}-\frac{d}{dZ}\frac{\partial\int_{-\infty}^{\infty}\mathscr{L}dt'}{\partial\mathbf{f}}=2\Re\int_{-\infty}^{\infty}\mathcal{Q}\frac{\delta\psi}{\delta\mathbf{f}} \quad (5)$$

in agreement with Kantorovitvh's method (see [15, 53, 55] and references herein).

Table 2. Normalizations for the LLE (2)

Value	Normalizations and definitions
(X,Y)	transverse coordinates, $(x,y)/w_T$
Z	propagation distance, z/ζ
t'	local time, $t/\sqrt{\lvert\beta_2\rvert\zeta}$
ζ	propagation scale, $k_0n_ow_T^2$
w_T	transverse scale, $\sqrt[4]{w_0^2/k_0^2n_0\delta}$
δ	GRIN contrast, n_1-n_0
$(k_0/2n_0)\left(n_1^2-n(x,y)^2\right)$	GRIN confining potential, $\simeq k_0\left(n_1-n(r)\right)$
$\lvert\psi\rvert^2$	intensity, $k_0n_2\zeta\lvert a\rvert^2$
Λ'	net-loss, $\Lambda-G_0$
Λ	averaged loss, LL_w/ζ
κ	spatial confinement parameter, G_0/w_p^2
ω	temporal confinement parameter, $G_0/\mathscr{T}^2$
$w_p\sqrt{G_0-\Lambda}$	soft aperture size
τ	squared inverse spectral filter, bandwidth normalized to $\lvert\beta_2\rvert\zeta$
k_0	wave-number, $2\pi/\lambda$
λ	central wavelength
n_1	GRIN core refractive index
n_0	GRIN cladding refractive index
n_2	nonlinear refractive index
L	loss coefficient
L_w	waveguide ("lattice") length
G_0 or $G(t=0,x=0,y=0)$	maximum saturated gain coefficient
w_p	pump beam size
$\mathscr{T}$	pump pulse width

It is convenient to assume the axial symmetry, which corresponds to the symmetry of a cylindrical waveguide, and transit to a radial coordinate $R = \sqrt{X^2 + Y^2}$. The next assumption is a Gaussian-sech approximation for an STDS profile:

$$\psi(Z,R,t') = \alpha(Z)\,\mathrm{sech}\left[\frac{t'}{\Upsilon(Z)}\right]\times \exp\left[i(\phi(Z)+\chi(Z)t'^2+\theta(Z)R^2)-\frac{R^2}{2\rho(Z)^2}\right], \quad (6)$$

where the $Z-$dependent STDS parameters of **f** in Eq. (5) are: α - amplitude, ϕ - phase, χ and θ are the temporal and spatial chirps, respectively; ρ and Υ are the beam size and STDS duration, respectively. After some algebraic manipulations, one can obtain the expressions for the steady-state (i.e., $Z-$independent) STDS parameters (the phase ϕ is irrelevant in our context):

$$\rho^2 = \frac{1}{384\pi^2\kappa\tau\Upsilon^2}\times \left[15\left(\sqrt{64\tau\left(30\tau-\pi^4\Upsilon^4\omega\right)+225}-15\right)- 64\tau\left(15\tau+2\pi^2\left(\tau+3\Lambda'\Upsilon^2\right)\right)\right], \quad (7)$$

$$\chi = \frac{\sqrt{\Upsilon^4\left(64\tau\left(30\tau-\pi^4\Upsilon^4\omega\right)+225\right)}-15\Upsilon^4}{16\pi^2\tau\Upsilon^4}, \quad (8)$$

$$\alpha_0^2 = \frac{-6\kappa^2\rho^8-6\rho^4+6}{2\rho^2},$$

$$\theta = -\frac{\kappa\rho^2}{2}.$$

The remaining equation for the STDS duration Υ

$$144\left(\pi^2-25\right)\tau^2+\left(16\left(3+\pi^2\right)\tau^2+45\right)\times \sqrt{64\tau\left(30\tau-\pi^4\Upsilon^4\omega\right)+225}+96\pi^4\Upsilon^4\omega+ +\frac{2^{13}3^3\pi^4\kappa\tau^3\Upsilon^4\left(-\frac{A^4}{3\times2^{15}\pi^8\kappa^2\tau^4\Upsilon^8}-\frac{3A^2}{2\pi^4\kappa^2\tau^2\Upsilon^4}+1\right)}{A}=675, \quad (9)$$

$$A = 64\tau\left(2\pi^2\left(3\Lambda'\Upsilon^2+\tau\right)+15\tau\right)- 15\left(\sqrt{64\tau\left(30\tau-\pi^4\Upsilon^4\omega\right)+225}-15\right) \quad (10)$$

must be solved numerically.

C. STDS parameters

Figs. 2-5 show the STDS width Υ and peak intensity α_0^2 obtained from Eqs. (7-9). Υ grows, and α_0^2 decreases with κ when a spectral dissipation τ is sufficiently low (Figs. 2, 3). Such a tendency corresponds to that of a DKLM regime with $\omega = 0$ and manifests the growth of spatial mode loss with an aperture squeezing [55].

In the vicinity of a "threshold" ($\Lambda' \to 0$), the additional longitudinal (3D) trapping defined by ω noticeably squeezes an STDS with the simultaneous peak power growth (Fig. 3). The additional solution branch in the region of small κ (Fig. 2) disappears with $\Lambda' \to 0$. In general, the STDS intensity growth and its width shortening with ω could result from an appearance of the external confinement along the $t-$ coordinate.

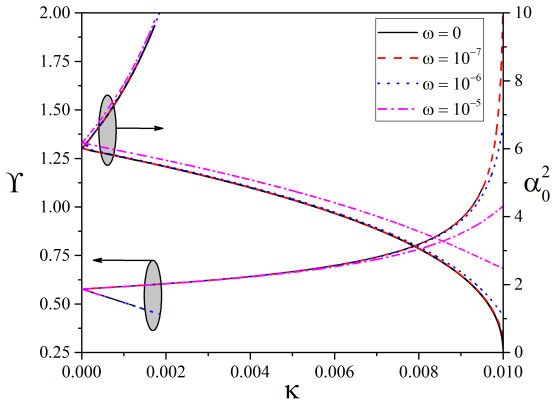

Fig. 2. Dimensionless pulse width Υ (left axis) and intensity α_0^2 (right axis) in dependence on the transverse (κ) and longitudinal (ω) gain grading parameters. Λ' =-0.01, τ =0.01.

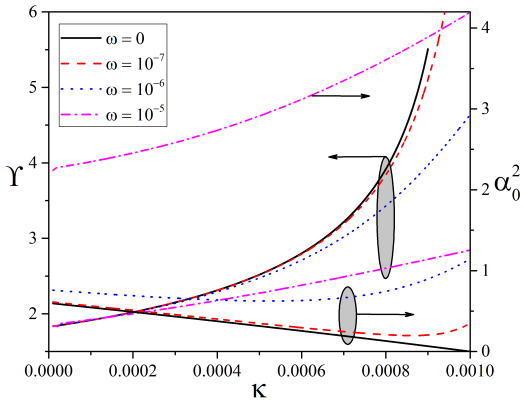

Fig. 3. Dimensionless pulse width Υ (left axis) and intensity α_0^2 (right axis) in dependence on the transverse (κ) and longitudinal (ω) gain grading parameters. $\Lambda' = -0.001$, τ =0.01.

The spectral dissipation increases with τ. That leads to an STDS collapse for $\kappa \to |\Lambda'|$ when the net-loss coefficient Λ' is more significant in comparison with Fig. 3. Such a collapse is asymmetrical in space and time. That is, STDS spreads along t and squeezes on R. A longitudinal mode selection growth with τ (i.e., STDS spreading in the time domain) parallels a transverse mode selection (STDS spatial squeezing) in the spatial domain.

The solutions bifurcate close to the threshold Λ' (Fig. 5). Such behavior leads to the thought of stability loss here. These oddities require numerical simulations of STDS dynamics presented below.

D. STDS stability

We performed large-scale numerical simulations of Eq. (2) based on the COMSOL Multiphysics software to analyze the stability of the analytical solutions based on the VA. The characteristic case is illustrated in Fig. 6, where the numerical STDS profile corresponds to one of the VA solutions from Fig. 4. The red line shows the analytical and numerical solutions shown by the black curve. One can see an oscillatory approach from the last

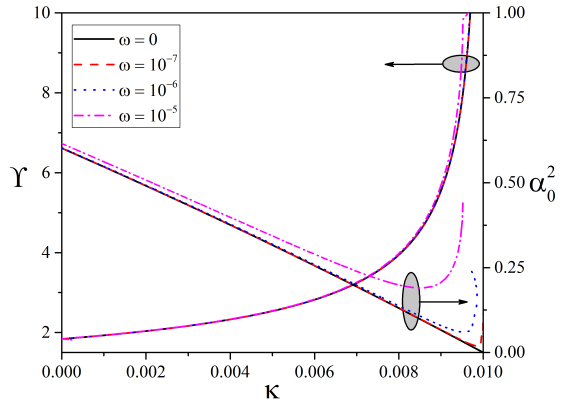

Fig. 4. Dimensionless pulse width Y (left axis) and intensity α_0^2 (right axis) in dependence on the transverse (κ) and longitudinal (ω) gain grading parameters. $\Lambda' = -0.01$, τ =0.1.

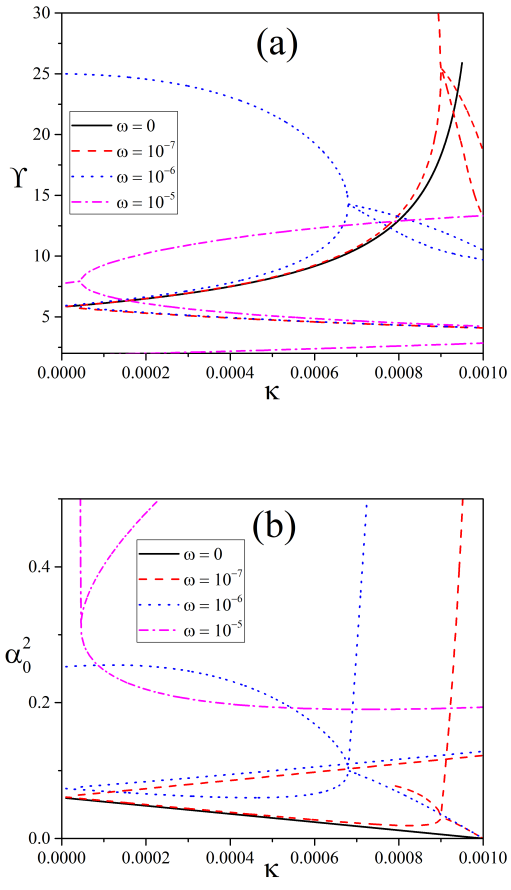

Fig. 5. Dimensionless pulse width Y (a) and intensity α_0^2 (b) in dependence on the transverse (κ) and longitudinal (ω) gain grading parameters. $\Lambda' = -0.001$, τ =0.1.

to the first, analogous to the damping of excitations in a weakly dissipative BEC [69]. Interestingly, the peak intensity of the numerical solution is slightly lower than the analytical one. The difference in the exact solution from the Gaussian ansatz for VA could explain it.

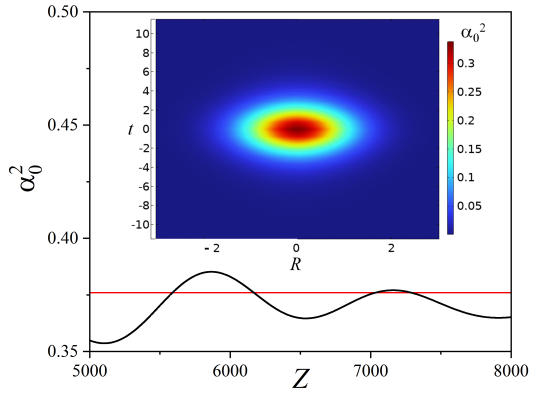

Fig. 6. Evolution of the STDS peak intensity α_0^2 (black solid curve) and its contour plot at Z =8000 (inset) for the parameters of Fig. 4 and ω =10^{-4}, κ =0.004. The red line shows the analytical α_0^2 from Fig. 4 for ω =10^{-4}, κ =0.004.

Besides the stable STDS solutions, the numerical simulations demonstrate three main destabilization scenarios. The first is the STDS decay with the $|\Lambda'|$-decrease. The second is the collapse-like behavior for small κ, ω, and τ. Both demonstrate the importance of dissipative factors (i.e., dissipative confinement and spectral filtering) for STDS stability.

The third scenario is the DS splitting with possible oscillations between multiple pulse states. Fig. 7 shows such regimes. The splitting in a local time domain could be explained by weaker confinement in the time domain due to lower ω. However, a more precise analysis of the STDS requires considering the gain saturation dynamics.

E. STDS stability under the saturable gain dynamics

To take into account the dynamical gain saturation, it is convenient to use the Frantz-Nodvik equation [70]:

$$\frac{\partial G_0}{\partial t} = \frac{G_{ss} - G_0}{T_r} - \frac{G_0 |\psi|^2}{E_s}, \tag{11}$$

where G_{ss} is a small signal gain, T_r is a gain relaxation time, $E_s = h\nu/S\sigma_{em}$ is a gain saturation energy (ν is a central gain-band wavelength coinciding with the STDS carrier frequency, S is a beam area, σ_{em} is a stimulated emission cross-section). Specifically, we base on the characteristics of the Cr:ZnS waveguide laser [71]. Table 3 presents the corresponding dimensional laser parameters.

The calculations demonstrate a visible effect of the gain saturation on the DS dynamics. For a small level of linear loss Λ, some characteristic profiles of STDS are shown in Fig. 8. As one can see, a sufficiently large ω stabilizes DS (a), but the driving frequency decrease leads to the STDS shape distortion, which is periodically asymmetrical along t-coordinate. Oscillations accompany these distortions and result in STDS decay. STDS

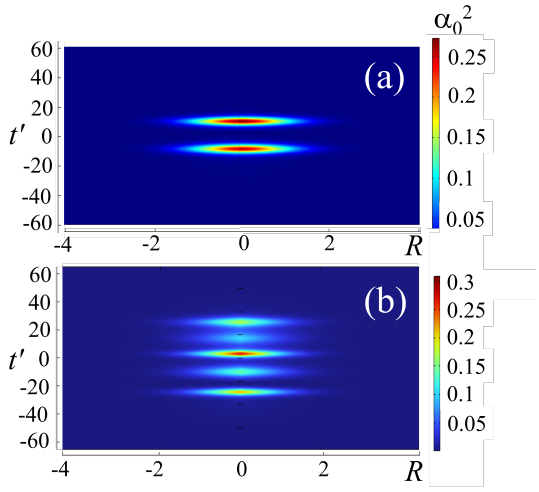

Fig. 7. Contour plot of the STDS peak intensity α_0^2 at Z =40000 (a) and 35000 (b) for $\omega = 10^{-5}$ (a) and 2×10^{-6} (b), κ =0.005, Λ' =-0.01, and τ =0.1.

cannot be stabilized for the parameters considered for a smaller Λ (Fig. 5).

The region of STDS stability is shown in Fig. 9 for a larger linear loss coefficient Λ. The STDS decay confines this region for larger κ, so there are no stable pulses for $\kappa \gtrsim 0.006$. The difference with the analytical results lies in the reduction of a net gain required for the soliton formation. Such a gain reduction is a direct consequence of the gain saturation. For smaller κ, the main destabilization factor is periodical pulse splitting, which alternates with a single-pulse regime (Figs. 8 (b-d) and inset in Fig. 9). The asymmetry of the STDS complex appears periodically due to dynamic gain saturation. When κ approaches zero, very strong STDS power and width oscillations appear. They reach more than two orders of magnitude, so STDS is periodically "reborn". This phenomenon confines the stability region from below on κ.

3. DISCUSSION AND CONCLUSION

Similar to the mechanism of STDS stabilization by non-dissipative confinement along the longitudinal (t) coordinate [53], which corresponds to an additive phase mode-locking in a laser, the dissipative confinement due to synchronous pulse pumping or active amplitude mode-locking leads to a stable STDS, as well. Such stabilization is possible at very low values of the modulation "depth" parameter $\omega = G_0/\mathcal{T}^2 \approx \Lambda/\mathcal{T}^2 \approx 10^{-4}$. This means that gain variations along a laser axis could be very small. For instance, it means that a pumping pulse, synchronized with the cavity round-trip, could be very "long" compared to the STDS temporal width. The contribution of dynamical gain saturation lowers this value to $\approx 10^{-6}$. Simultaneously, there is a lower threshold on the value of the saturated net gain $|\Lambda'|$. In our case, it was ≈ 0.01. Too low net gain could not provide the 3D dissipative confinement and, thereby, STDS stabilization. We also found that the most optimal stabilization region is located near $\kappa \approx |\Lambda'|/2$. Considering the dynamical gain saturation, the corresponding value is $\kappa \approx \Lambda/4 - \Lambda/3$. It is important that spectral dissipation (τ) is required for STDS stabilization. One may assume that the too-low value of this parameter cannot prevent a tendency to the STDS collapse.

Table 3. Correspondences between photonics and BEC

Cr:ZnS laser parameters (see Table 1)	values
gain relaxation time T_r, μs	4.9
gain cross-section σ_{em}, cm^2	$1.38{\cdot}10^{-18}$
coefficient of nonlinear refraction n_2, cm^2 W^{-1}	$9{\cdot}10^{-15}$
central wavelength λ, μm	2.3
w_0, μm	40
n_0	2.2629
δ	0.0077
numerical aperture $NA = \sqrt{n_1^2 - n_0^2}$	≈ 0.19
w_T, cm	0.001
ζ, cm	0.03
$S = \pi w_0^2/2$, cm^2	$2.5{\cdot}10^{-5}$
β_2, fs^2/cm	1280

The numerical simulations demonstrated that, besides the STDS destabilization due to decay for low $|\Lambda'|, \kappa \to 0 \wedge |\Lambda'|$, and small ω and τ, there is a tendency to STDS splitting in the time domain with the growth of κ if ω is not sufficiently high. That means a "transverse" confinement needs an adequate "longitudinal" one. Despite the case of longitudinal phase confinement [53], we did not observe complicated spatial dynamics and splitting that testifies to the intensification of the mode cleaning process. Although "ring-like" spatial structures and the STDS "breathing" in the transverse direction are possible in the initial stages of evolution.

We found that the gain saturation could significantly impact the STDS dynamics. For the considered values of gain coefficient G_{ss} there is a confined range of driving frequency ω providing the STDS stability, and this region is the broadest in the vicinity of $\kappa \approx 0.0003 - 0.0004$. The main mechanism of destabilization is STDS decay. A possible explanation is the following. Too small ω does not provide sufficient confinement along $t-$dimension for a chosen G_{ss}. Too large driven frequency squeezes a gain window so STDS cannot be amplified sufficiently to start a Kerr effect for spatial squeezing, and spatial confinement becomes destructive. Also, the dynamical gain saturation defines some maximum κ because it decreases an effective gain, and the spatial losses lead to the STDS decay. STDS peak power and width oscillations appear for small κ. These oscillations can be extremely strong and accompanied by alternating between asymmetric one and two pulses.

We must note, that the cavity round-trip period could excess essentially $2L_w/c$ in order to provide the STDS energy scalability [59]. This method is practiced in high-energy passively mode-locked oscillators (e.g., see [12, 30]). In a waveguide oscillator, it is possible to use the Herriott cell or fiber loop for this aim. The last approach could be the most effective for the STDS generation in a fiber laser [53].

In conclusion, we propose a mechanism of STDS stabilization using longitudinally and transversely graded gain in a waveguide laser with transversely graded refractive index and Kerr nonlinearity. Practically, that means realizing a DKLM in a waveguide laser operating in ADR and pumped by a Gaussian

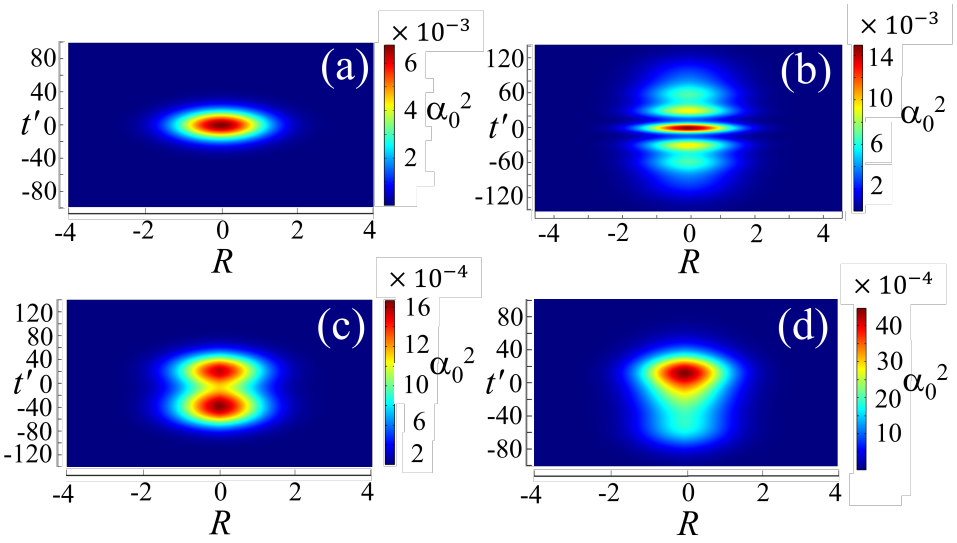

Fig. 8. Contour plots of the STDS peak intensity α_0^2. $\omega = 5 \times 10^{-6}$, $Z = 7 \times 10^4$ (a), and $\omega = 5 \times 10^{-7}$ (b–d) for different lengths of propagation. κ =0.005, Λ =0.01, G_{ss} =1.1Λ, and τ =0.1. GDD is anomalous.

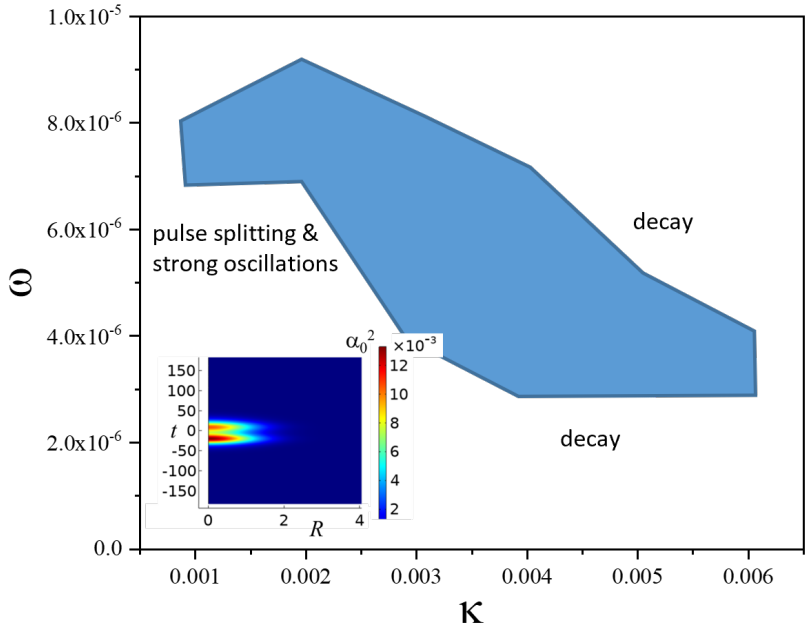

Fig. 9. Region of STDS stability on (κ–ω)-plane under the action of dynamical gain saturation. Λ =0.1, and other parameters as in Fig. 8. Inset shows the $|\alpha_0|^2$ contour plot for $\kappa = 5 \times 10^{-4}$, $\omega = \times 10^{-6}$.

beam with slow amplitude temporal modulation synchronized with a laser repetition rate. In some sense, that is a dissipative analog of "pancake-like" confining potential in a weakly dissipative BEC. The analytical solutions for such STDS are obtained in the framework of VA depending on the parameters of the pump beam, such as its width, modulation depth, and saturated net gain. The essential ingredient of our model is spectral dissipation due to finite spectral gain bandwidth, which contributes to STDS stabilization. Numerical simulations under cylindrical symmetry conditions demonstrate the STDS's stability within a limited region of parameters defined by net gain, pump beam width, and spectral bandwidth. Considering the dynamical gain saturation, we defined the main destabilization scenarios: decay and STDS oscillations asymmetrically alternating one and two pulses. We assume that the self-control of the transverse modes by the combination of enhanced nonlinearity, specific for the distributed nonlinear systems like waveguides composed from highly-nonlinear media, with the dissipative confinement, could

provide the breakthrough in developing the new generation of high-stable and energy scalable sources of STDS. In principle, this approach is a further development of the DKLM concept that proved its efficiency for energy-scalable solid-state lasers. Moreover, it could be useful for stabilizing other localized coherent structures, e.g., a weakly dissipative BEC.

FUNDING

The Norwegian Research Council projects #303347 (UNLOCK), #326503 (MIR), #32641 (Lammo-3D), and ALTA Lasers AS supported this work.

REFERENCES

1. P. G. Kevrekidis, D. J. Frantzeskakis, and C.-G. R., *Emergent Nonlinear Phenomena in Bose-Einstein Condensates: Theory and Experiment* (Springer, Berlin Heidelberg, 2008).
2. Z.-H. Luo, W. Pang, B. Liu, Y.-Y. Li, and B. A. Malomed, "A new form of liquid matter: Quantum droplets," Front. Phys. **16**, 1–21 (2021).
3. M. Cazalilla, R. Citro, T. Giamarchi, E. Orignac, and M. Rigol, "One dimensional bosons: From condensed matter systems to ultracold gases," Rev. Mod. Phys. **83**, 1405 (2011).
4. R. Carretero-González, D. Frantzeskakis, and P. Kevrekidis, "Nonlinear waves in bose–einstein condensates: physical relevance and mathematical techniques," Nonlinearity. **21**, R139 (2008).
5. M. Boninsegni and N. V. Prokof'ev, "Colloquium: Supersolids: What and where are they?" Rev. Mod. Phys. **84**, 759 (2012).
6. P. Robinson, "Nonlinear wave collapse and strong turbulence," Rev. modern physics **69**, 507 (1997).
7. A. Dyachenko, V. Zakharov, A. Pushkarev, V. Shvets, and V. Yankov, "Soliton turbulence in nonintegrable wave systems," Zh. Eksp. Teor. Fiz **96**, 19 (1989).
8. E. Kuznetsov, A. Rubenchik, and V. E. Zakharov, "Soliton stability in plasmas and hydrodynamics," Phys. Reports **142**, 103–165 (1986).
9. F. Krausz and M. Ivanov, "Attosecond physics," Rev. modern physics **81**, 163 (2009).
10. G. A. Mourou, T. Tajima, and S. V. Bulanov, "Optics in the relativistic regime," Rev. modern physics **78**, 309 (2006).
11. R. J. England, R. J. Noble, K. Bane, D. H. Dowell, C.-K. Ng, J. E. Spencer, S. Tantawi, Z. Wu, R. L. Byer, E. Peralta *et al.*, "Dielectric laser accelerators," Rev. Mod. Phys. **86**, 1337 (2014).
12. T. Südmeyer, S. Marchese, S. Hashimoto, C. Baer, G. Gingras, B. Witzel, and U. Keller, "Femtosecond laser oscillators for high-field science," Nat. photonics **2**, 599–604 (2008).
13. A. Gallerati, G. Modanese, and G. A. Ummarino, "Interaction between macroscopic quantum systems and gravity," Front. Phys. p. 559 (2022).
14. D. Faccio, "Laser pulse analogues for gravity and analogue hawking radiation," Contemp. Phys. **53**, 97–112 (2012).
15. V. Kalashnikov and S. Wabnitz, "A "metaphorical" nonlinear multimode fiber laser approach to weakly dissipative bose-einstein condensates a," Europhys. Lett. **133**, 34002 (2021).
16. D. Faccio, S. Cacciatori, V. Gorini, V. Sala, A. Averchi, A. Lotti, M. Kolesik, and J. Moloney, "Analogue gravity and ultrashort laser pulse filamentation," EPL (Europhysics Lett. **89**, 34004 (2010).
17. D. V. Averin, B. Ruggiero, and P. Silvestrini, *Macroscopic quantum coherence and quantum computing* (Springer Science & Business Media, 2012).
18. P. Forn-Díaz, L. Lamata, E. Rico, J. Kono, and E. Solano, "Ultrastrong coupling regimes of light-matter interaction," Rev. Mod. Phys. **91**, 025005 (2019).
19. R. R. Gattass and E. Mazur, "Femtosecond laser micromachining in transparent materials," Nat. photonics **2**, 219–225 (2008).
20. D. Andrews, G. Scholes, and G. Wiederrecht, *Comprehensive nanoscience and technology* (Academic Press, 2010).
21. A. Y. Vorobyev and C. Guo, "Direct femtosecond laser surface nano/microstructuring and its applications," Laser & Photonics Rev. **7**, 385–407 (2013).
22. M. C. Cross and P. C. Hohenberg, "Pattern formation outside of equilibrium," Rev. modern physics **65**, 851 (1993).
23. W. Fu, L. G. Wright, P. Sidorenko, S. Backus, and F. W. Wise, "Several new directions for ultrafast fiber lasers," Opt. express **26**, 9432–9463 (2018).
24. H.-G. Purwins, H. Bödeker, and S. Amiranashvili, "Dissipative solitons," Adv. Phys. **59**, 485–701 (2010).
25. N. Akhmediev and A. Ankiewicz, *Dissipative solitons: from optics to biology and medicine*, vol. 751 (Springer Science & Business Media, 2008).
26. T. Brabec and F. Krausz, "Intense few-cycle laser fields: Frontiers of nonlinear optics," Rev. Mod. Phys. **72**, 545 (2000).
27. P. Grelu and N. Akhmediev, "Dissipative solitons for mode-locked lasers," Nat. photonics **6**, 84–92 (2012).
28. J. Brons, "High-power femtosecond laser-oscillators for application in high-field physics," Ph.D. thesis, Ludwig Maximilians Universität München (2017).
29. I. T. Sorokina, E. Sorokin, E. Wintner, A. Cassanho, H. P. Jenssen, and M. A. Noginov, "Efficient continuous-wave tem00 and femtosecond kerr-lens mode-locked cr:lisrgaf laser," Opt. Lett. **21**, 204–206 (1996).
30. J. Zhang, M. Poetzlberger, Q. Wang, J. Brons, M. Seidel, D. Bauer, D. Sutter, V. Pervak, A. Apolonski, K. F. Mak *et al.*, "Distributed kerr lens mode-locked yb: Yag thin-disk oscillator," Ultrafast Sci. **2022** (2022).
31. M. Demesh, V. L. Kalashnikov, E. Sorokin, N. Gusakova, A. Rudenkov, and I. T. Sorokina, "At the threshold of distributed kerr-lens mode-locking in a cr:zns waveguide laser," J. Opt. Soc. Am. B **40**, 1717–1725 (2023).
32. T. Brabec, C. Spielmann, P. Curley, and F. Krausz, "Kerr lens mode locking," Opt. letters **17**, 1292–1294 (1992).
33. C. R. Baer, O. H. Heckl, C. J. Saraceno, C. Schriber, C. Kränkel, T. Südmeyer, and U. Keller, "Frontiers in passively mode-locked high-power thin disk laser oscillators," Opt. Express **20**, 7054–7065 (2012).
34. O. Pronin, J. Brons, C. Grasse, V. Pervak, G. Boehm, M.-C. Amann, A. Apolonski, V. L. Kalashnikov, and F. Krausz, "High-power kerr-lens mode-locked yb: Yag thin-disk oscillator in the positive dispersion regime," Opt. letters **37**, 3543–3545 (2012).
35. V. L. Kalashnikov, *Chirped-pulse oscillators: route to the energy-scalable femtosecond pulses* (InTech Croatia, 2012).
36. W. Chang, A. Ankiewicz, J. Soto-Crespo, and N. Akhmediev, "Dissipative soliton resonances," Phys. Rev. A **78**, 023830 (2008).
37. F. W. Wise, A. Chong, and W. H. Renninger, "High-energy femtosecond fiber lasers based on pulse propagation at normal dispersion," Laser & Photonics Rev. **2**, 58–73 (2008).
38. P. Mondal, V. Mishra, and S. K. Varshney, "Nonlinear interactions in multimode optical fibers," Opt. Fiber Technol. **54**, 102041 (2020).
39. M. Piccardo, V. Ginis, A. Forbes, S. Mahler, A. A. Friesem, N. Davidson, H. Ren, A. H. Dorrah, F. Capasso, F. T. Dullo *et al.*, "Roadmap on multimode light shaping," J. Opt. **24**, 013001 (2021).
40. M. Matuszewski, E. Infeld, B. A. Malomed, and M. Trippenbach, "Stabilization of three-dimensional light bullets by a transverse lattice in a kerr medium with dispersion management," Opt. communications **259**, 49–54 (2006).
41. Y. V. Kartashov, B. A. Malomed, and L. Torner, "Solitons in nonlinear lattices," Rev. Mod. Phys. **83**, 247 (2011).
42. L. G. Wright, D. N. Christodoulides, and F. W. Wise, "Spatiotemporal mode-locking in multimode fiber lasers," Science. **358**, 94–97 (2017).
43. L. G. Wright, P. Sidorenko, H. Pourbeyram, Z. M. Ziegler, A. Isichenko, B. A. Malomed, C. R. Menyuk, D. N. Christodoulides, and F. W. Wise, "Mechanisms of spatiotemporal mode-locking," Nat. Phys. **16**, 565–570 (2020).
44. A. Siegman, "Propagating modes in gain-guided optical fibers," JOSA A **20**, 1617–1628 (2003).
45. Y. Sun, P. Parra-Rivas, C. Milián, Y. V. Kartashov, M. Ferraro, F. Mangini, R. Jauberteau, F. R. Talenti, and S. Wabnitz, "Robust three-dimensional high-order solitons and breathers in driven dissipative systems: a kerr cavity realization," Phys. Rev. Lett. **131**, 137201 (2023).
46. Z. Li, Y. Xu, S. Shamailov, X. Wen, W. Wang, X. Wei, Z. Yang, S. Coen, S. G. Murdoch, and M. Erkintalo, "Ultrashort dissipative raman solitons

in kerr resonators driven with phase-coherent optical pulses," arXiv preprint arXiv:2212.08223 (2022).
47. E. Kengne, W.-M. Liu, and B. A. Malomed, "Spatiotemporal engineering of matter-wave solitons in bose–einstein condensates," Phys. Reports **899**, 1–62 (2021).
48. N. Smith, K. Blow, W. Firth, and K. Smith, "Soliton dynamics in the presence of phase modulators," Opt. communications **102**, 324–328 (1993).
49. S. Wabnitz, "Suppression of soliton interactions by phase modulation," Electron. Lett. **19**, 1711–1713 (1993).
50. W. Chang, N. Akhmediev, S. Wabnitz, and M. Taki, "Influence of external phase and gain-loss modulation on bound solitons in laser systems," JOSA B **26**, 2204–2210 (2009).
51. F. Leo, S. Coen, P. Kockaert, S.-P. Gorza, P. Emplit, and M. Haelterman, "Temporal cavity solitons in one-dimensional kerr media as bits in an all-optical buffer," Nat. Photonics **4**, 471–476 (2010).
52. N. Englebert, N. Goldman, M. Erkintalo, N. Mostaan, S.-P. Gorza, F. Leo, and J. Fatome, "Bloch oscillations of driven dissipative solitons in a synthetic dimension," arXiv preprint arXiv:2112.10756 (2021).
53. V. L. Kalashnikov and S. Wabnitz, "Stabilization of spatiotemporal dissipative solitons in multimode fiber lasers by external phase modulation," Laser Phys. Lett. **19**, 105101 (2022).
54. Y. Zhu, B. Semisalov, and S. Krstulovic, G.and Nazarenko, "Testing wave turbulence theory for the gross-pitaevskii system," Phys. Rev. E **106**, 014205 (2022).
55. V. L. Kalashnikov and S. Wabnitz, "Distributed kerr-lens mode locking based on spatiotemporal dissipative solitons in multimode fiber lasers," Phys. Rev. A **102**, 023508 (2020).
56. V. Skarka, N. Aleksić, H. Leblond, B. Malomed, and D. Mihalache, "Varieties of stable vortical solitons in ginzburg-landau media with radially inhomogeneous losses," Phys. review letters **105**, 213901 (2010).
57. V. E. Lobanov, O. V. Borovkova, Y. V. Kartashov, V. A. Vysloukh, and L. Torner, "Topological light bullets supported by spatiotemporal gain," Phys. Rev. A **85**, 023804 (2012).
58. S. A. Akhmanov, V. A. Vysloukh, A. S. Chirkin, and Y. Atanov, *Optics of femtosecond laser pulses* (Springer, 1992).
59. M. Demesh, V. L. Kalashnikov, E. Sorokin, N. Gusakova, A. Rudenkov, and I. T. Sorokina, "At the threshold of distributed kerr-lens modelocking in a cr:zns waveguide laser," J. Opt. Soc. Am. B **40**, 1717–1725 (2023).
60. L. Lugiato, F. Prati, and M. Brambilla, *Nonlinear optical systems* (Cambridge University Press, 2015).
61. F. Castelli, M. Brambilla, A. Gatti, F. Prati, and L. A. Lugiato, "The lle, pattern formation and a novel coherent source," The Eur. Phys. J. D **71**, 1–16 (2017).
62. L. Lugiato, F. Prati, M. Gorodetsky, and T. Kippenberg, "From the lugiato–lefever equation to microresonator-based soliton kerr frequency combs," Philos. Transactions Royal Soc. A: Math. Phys. Eng. Sci. **376**, 20180113 (2018).
63. S. Coen and M. Erkintalo, "Temporal cavity solitons in kerr media," Nonlinear Opt. Cavity Dyn. From Microresonators to Fiber Lasers pp. 11–40 (2016).
64. L. A. Lugiato and R. Lefever, "Spatial dissipative structures in passive optical systems," Phys. review letters **58**, 2209 (1987).
65. M. Haelterman, S. Trillo, and S. Wabnitz, "Dissipative modulation instability in a nonlinear dispersive ring cavity," Opt. communications **91**, 401–407 (1992).
66. P. Aschieri, J. Garnier, C. Michel, V. Doya, and A. Picozzi, "Condensation and thermalization of classsical optical waves in a waveguide," Phys. Rev. A **83**, 033838 (2011).
67. S. Raghavan and G. P. Agrawal, "Spatiotemporal solitons in inhomogeneous nonlinear media," Opt. Commun. **180**, 377–382 (2000).
68. J. Herrmann and B. Wilhelmi, "Lasers for ultrashort light pulses," in *Lasers for Ultrashort Light Pulses,* (North-Holland, Amsterdam, 1987).
69. S. Choi, S. Morgan, and K. Burnett, "Phenomenological damping in trapped atomic bose-einstein condensates," Phys. Rev. A **57**, 4057 (1998).
70. L. M. Frantz and J. S. Nodvik, "Theory of pulse propagation in a laser amplifier," J. applied physics **34**, 2346–2349 (1963).
71. E. Sorokin, A. A. Bushunov, N. Tolstik, A. A. Teslenko, E. Einmo, M. K. Tarabrin, V. A. Lazarev, and I. T. Sorokina, "All-laser-microprocessed waveguide cr: Zns laser," Opt. Mater. Express **12**, 414–420 (2022).